

phys. stat. sol. (a) **59**, 121 (1980)

Subject classification: 20.2 and 20.3; 22.8.1

A. V. Shubnikov Institute of Crystallography, Academy of Sciences of the USSR, Moscow¹ (a), Institute of Geology and Geophysics, Academy of Sciences of the USSR, Novosibirsk (b), and P. N. Lebedev Physical Institute, Academy of Sciences of the USSR, Moscow (c)

Growth, Spectral and Laser Properties of $\text{La}_2\text{Be}_2\text{O}_5:\text{Nd}^{3+}$ Crystals in the ${}^4\text{F}_{3/2} \rightarrow {}^4\text{I}_{11/2}$ and ${}^4\text{F}_{3/2} \rightarrow {}^4\text{I}_{13/2}$ Transitions

By

A. A. KAMINSKII (a), TRAN NGOC (a), S. E. SARKISOV (a), V. N. MATROSOV (b),
and M. I. TIMOSHECHKIN (c)

Detailed investigations of intermanifold luminescence intensity anisotropy in the main ${}^4\text{F}_{3/2} \rightarrow {}^4\text{I}_{11/2}$ and additional ${}^4\text{F}_{3/2} \rightarrow {}^4\text{I}_{13/2}$ channels of the Nd^{3+} ion in $\text{La}_2\text{Be}_2\text{O}_5$ crystals are carried out for three crystallographic orientations *a*, *b*, and *c* at 77 and 300 K. Orientational values of main spectroscopic characteristics, including Stark luminescence branching ratios β_{ij}^{or} , peak and effective cross-sections ($\sigma_{e,ij}^{\text{or}}$ and σ_e^{eff}) of the transitions, at the wavelengths of which stimulated emission is excited, are determined for the ${}^4\text{F}_{3/2} \rightarrow {}^4\text{I}_{11/2,13/2}$ channels. The temperature behaviour of laser lines in the $\text{La}_2\text{Be}_2\text{O}_5:\text{Nd}^{3+}$ (*F* || *c*) crystals is studied for the ${}^4\text{F}_{3/2} \rightarrow {}^4\text{I}_{11/2}$ channel in the temperature region of 77 to 300 K. Reswitching of laser lines, 1.0694 and 1.0785 μm , is observed in the temperature region of liquid nitrogen. The explanation of this effect is done on the basis of spectroscopic investigations. The energy of Stark levels of Nd^{3+} ions in $\text{La}_2\text{Be}_2\text{O}_5$ crystals is refined and all excited laser lines are identified. Preliminary analysis of spectroscopic properties is carried out for Pr^{3+} ions in $\text{La}_2\text{Be}_2\text{O}_5$ and the crystal-field splitting scheme is defined for the manifolds, transitions among levels of which correspond to the optical transparency band of $\text{La}_2\text{Be}_2\text{O}_5$ crystals.

Проведены детальные исследования анизотропии пространственного распределения интенсивностей межмультиплетной люминесценции на основном ${}^4\text{F}_{3/2} \rightarrow {}^4\text{I}_{11/2}$ и дополнительном ${}^4\text{F}_{3/2} \rightarrow {}^4\text{I}_{13/2}$ каналах иона Nd^{3+} в кристаллах $\text{La}_2\text{Be}_2\text{O}_5$ для трех кристаллографических направлений *a*, *b* и *c* при 77 и 300 К. Определены ориентационные значения основных спектроскопических характеристик, включая „штарковские“ коэффициенты ветвления люминесценции β_{ij}^{or} , пиковые и эффективные поперечные сечения ($\sigma_{e,ij}^{\text{or}}$ и σ_e^{eff}) переходов, на длинах волн которых возбуждено стимулированное излучение в каналах ${}^4\text{F}_{3/2} \rightarrow {}^4\text{I}_{11/2,13/2}$. Изучено температурное поведение линий генерации кристаллов $\text{La}_2\text{Be}_2\text{O}_5:\text{Nd}^{3+}$ (*F* || *c*) в канале ${}^4\text{F}_{3/2} \rightarrow {}^4\text{I}_{11/2}$ в интервале температур 77 до 300 К. Обнаружено переключение линий генерации 1,0694 и 1,0785 μm в области температур жидкого азота. Дано объяснение этого эффекта на основании результатов спектроскопических исследований. Уточнена энергия штарковских уровней иона Nd^{3+} в кристалле $\text{La}_2\text{Be}_2\text{O}_5$ и идентифицированы все возбужденные его лазерные линии. Проведен предварительный анализ спектроскопических свойств иона Pr^{3+} в $\text{La}_2\text{Be}_2\text{O}_5$ и построена схема кристаллического расщепления мультиплетов, переходы между уровнями которых попадают в окно оптической прозрачности кристалла.

¹) Leninskii prospekt 59, 117333 Moscow, USSR.

1. Introduction

The perspectives of monoclinic $\text{La}_2\text{Be}_2\text{O}_5:\text{Nd}^{3+}$ crystals as laser media are shown in [1 to 3], where stimulated emission (SE) at the lines of the main ${}^4\text{F}_{3/2} \rightarrow {}^4\text{I}_{11/2}$ transition was studied in different generation regimes. In particular, in these detailed investigations it was determined that $\text{La}_2\text{Be}_2\text{O}_5:\text{Nd}^{3+}$ crystals in comparison with $\text{Y}_3\text{Al}_5\text{O}_{12}:\text{Nd}^{3+}$ give higher output energies (approximately by three times) in the Q-switched operation [2] and shorter pulses (by 2 to 3 times) in the passive mode-locking performance [3]. The SE wavelength of the $\text{La}_2\text{Be}_2\text{O}_5:\text{Nd}^{3+}$ crystals in the ${}^4\text{F}_{3/2} \rightarrow {}^4\text{I}_{11/2}$ transition with $\lambda_g = 1.0698 \mu\text{m}$ was refined and generation in the additional ${}^4\text{F}_{3/2} \rightarrow {}^4\text{I}_{13/2}$ transition with $\lambda_g = 1.3510 \mu\text{m}$ was excited first by us in [4]. The compound $\text{La}_2\text{Be}_2\text{O}_5$ was first reported by Weir and Van Valkenburg in 1960 [5], who established its formula on the basis of solid-state synthesis and listed optical and powder X-ray diffraction data. The crystal structure was determined by Harris and Yakel [6]. The first information on the growth of single $\text{La}_2\text{Be}_2\text{O}_5:\text{Nd}^{3+}$ crystals and the first data on their spectroscopic properties were reported in [7]. In the cited papers as well as in [8, 9] a number of important physical parameters of the $\text{La}_2\text{Be}_2\text{O}_5$ crystal were measured, which are listed in Table 1 for complete information.

The present work deals with complex investigations of luminescence and laser characteristics in anisotropic $\text{La}_2\text{Be}_2\text{O}_5:\text{Nd}^{3+}$ crystals at 77 and 300 K. The main problems of the work are the determination of the orientational (over three crystallographic axes a , b , and c) intermanifold ${}^4\text{F}_{3/2} \rightarrow {}^4\text{I}_{J'}$ and Stark luminescence branching ratios ($\beta_{J'J''}^{\text{or}}$ and β_{ij}^{or}), measurement of peak and effective cross-sections ($\sigma_{e,ij}^{\text{or}}$ and σ_e^{eff}) of the transitions among ${}^4\text{F}_{3/2}$, ${}^4\text{I}_{11/2,13/2}$ manifolds. The investigations of SE temperature behaviour and the problem of reswitching of the SE lines in the ${}^4\text{F}_{3/2} \rightarrow {}^4\text{I}_{11/2}$ channel at temperatures of liquid nitrogen are discussed. Preliminary spectroscopic investigations of the $\text{La}_2\text{Be}_2\text{O}_5:\text{Pr}^{3+}$ crystals were also carried out and allowed to determine the crystal-field splitting scheme of all Pr^{3+} ion manifolds in the optical transparency band of the $\text{La}_2\text{Be}_2\text{O}_5$ crystal.

2. Crystal Growth and Samples for Investigations

The $\text{La}_2\text{Be}_2\text{O}_5$ crystals were grown either from the preliminary synthesized starting material or from the melt, obtained directly by co-melting BeO and La_2O_3 oxides. Beryllium oxide of 99.999% purity and lanthanum oxide of 99.99% purity²⁾ were used in the experiments. The Czochralski techniques with r.f. heating using platinum and rhodium crucibles was employed. The growth was carried out in air, argon, and in a mixed argon/air controlled atmosphere at a chamber pressure of 1.2 to 1.8 atm. Growth experiments showed that Tyndall scattering caused by inclusions of Pt particles are the main defect of the $\text{La}_2\text{Be}_2\text{O}_5$ crystals grown from Pt crucibles. Particles are included into the central part of the crystal over the entire length, where the linear rotation rate is very small. The defect diameter is in the region from 0.1 to 1 to 2 mm, and mainly depends on the composition and the pressure in the crystallization chamber. This defect is maximum in a crystal grown in air and in air/argon atmosphere and is reduced to 0.1 to 0.3 mm at 1.8 atm Ar pressure. Such formation of the inclusions depends also on the melting level in the crucible, especially when the volume decreased to lower than the half of the crucible. In the $\text{La}_2\text{Be}_2\text{O}_5$ crystals grown from Rh crucibles the mentioned defect due to particle inclusion was absent in Ar atmosphere. The optimum growth regime for the $\text{La}_2\text{Be}_2\text{O}_5:\text{Nd}^{3+}$ (1 wt%) single crystals of ≈ 20 mm in diameter was the following: pulling rate 1.5 to 2.0 mm/h and rotation

²⁾ BeO of "OCY" and La_2O_3 of "Y" types (Soviet trade marks).

35 to 40 min^{-1} . Some additional information on the $\text{La}_2\text{Be}_2\text{O}_5:\text{Nd}^{3+}$ crystal growth can be found in [1, 7, 8].

A single-block rectangular sample of $8 \times 9 \times 10 \text{ mm}^3$ cut from a $\text{La}_2\text{Be}_2\text{O}_5:\text{Nd}^{3+}$ (≈ 1 at%) crystal of high optical homogeneity ($\Delta n \leq 10^{-4}$) with the sides perpendicular (with an accuracy of about 2°) to the crystallographic axes a , b , and c was used for spectroscopic experiments. In laser experiments $\text{La}_2\text{Be}_2\text{O}_5:\text{Nd}^{3+}$ (or Pr^{3+}) crystal rods (1 at% Nd_2O_3 or Pr_2O_3) ≈ 70 mm in length and 6 mm in diameter with plane-parallel ends ($\approx 10''$) were used.

3. Experimental Technique and Investigation Methods

All spectroscopic measurements connected with the determination of Stark level energies and with the identification of transitions among these levels were carried out by traditional methods (absorption and luminescence analysis) and SE spectroscopy methods. In these experiments high resolution spectral apparatus (such as DFS-8, DFS-12, SDL-1, Specord 75-IR, and MDR-3 monochromator with 200 grooves/mm grating) were used. Effective illuminating systems using quartz tungsten-iodine lamp of KGM-12-100 type and Ar laser of LG-106M-1 type were employed for luminescence excitation. The spectral line intensity (by spectroscopic quality parameter X) was determined on the base of a modified Judd-Ofelt method (cf. [10, 11]) using a SF-8 spectrophotometer. The orientational luminescence spectra with high accuracy were recorded on a SDL-1 grating spectrometer, which was energy calibrated by the emission of a special standard tungsten lamp with colour temperature of 2850 K. It should be noted that all possible luminescence excitation cases realized during the pumping of a crystal in the real lasers, i.e. isotropic cylindrical and anisotropic excitation cases, were taken into consideration. But, as our investigations show, the relative redistribution of the intermanifold luminescence intensity for crystallographic orientations a , b , and c of the $\text{La}_2\text{Be}_2\text{O}_5:\text{Nd}^{3+}$ crystals weakly depends on the luminescence excitation direction and practically is within the experimental accuracy ($\pm 10\%$). The investigation of SE temperature behaviour was carried out using experimental techniques described in [12 to 14]. A confocal resonator formed by two external spherical multilayer mirrors ($R = 600$ mm) with transparency about 1% at the lasing wavelength was used in laser experiments. A monochromator ZMR-3 and stroboscopic lamp of ISSh-100-3 type were used for luminescence decay measurements. The intermanifold luminescence branching ratios $\beta_{JJ'}^{\text{or}}$ were determined from the orientational luminescence spectra by the method described in [12]. Their values give the spatial distribution of the anisotropy of intermanifold transition intensities from the metastable ${}^4\text{F}_{3/2}$ state of Nd^{3+} ions in the crystals. The connection of $\beta_{JJ'}^{\text{or}}$ and Stark β_{ij}^{or} with intermanifold luminescence branching ratios $\beta_{JJ'}$, which were determined using the parameter X mentioned above, is expressed by the following formula:

$$\beta_{JJ'} = \frac{1}{3} \sum_{a,b,c} \beta_{JJ'}^{\text{or}} = \frac{1}{3} \sum_{ij} \sum_{a,b,c} \beta_{ij}^{\text{or}}, \quad (1)$$

where the summation is carried out over all Stark $i \rightarrow j$ transitions of a given $J \rightarrow J'$ channel and along the three crystallographic axes a , b , and c .

The orientational peak and effective cross-sections of the ${}^4\text{F}_{3/2} \rightarrow {}^4\text{I}_{11/2,13/2}$ channel transitions were calculating according to the formulae

$$\sigma_{e,ij}^{\text{or}} = \frac{\lambda_{ij}^2}{4\pi^2 n^2} \frac{\beta_{ij}^{\text{or}}}{\Delta\nu_{\text{lum}} \tau_{\text{rad}}} = \frac{\lambda_{ij}^2}{4\pi^2 n^2} \frac{A_{ij}^{\text{or}}}{b_i} \quad (2)$$

and

$$\sigma_e^{\text{eff}} = \sigma_{e,ij}^{\text{or}} + \sum_{(imjm) \neq (ij)} p_{ij}^{imjm} \sigma_{e,imjm}^{\text{or}}, \quad (3)$$

respectively. In this form, $\sigma_{e,ij}^{\text{or}}$ and σ_e^{eff} values take into account the initial level (i) population and characterize the real intensity of a luminescent line at a given temperature and along a chosen direction of the luminescence observation. In (2) and (3) λ_{ij} is the wavelength of the $i \rightarrow j$ transition, n the refractive index (taken as orientationally independent, see Table I), A_{ij}^{or} the orientational spontaneous emission prob-

Table 1

Physical properties of $\text{La}_3\text{Be}_2\text{O}_5$ crystal at 300 K [2, 6, 9]

space group	$C_{2h}^6 - C2/c$
lattice constants (Å)	$a_0 = 7.5356$ $b_0 = 7.3476$ $c_0 = 7.4387$
angle between crystallographic axes a and c	$\beta = 91^\circ 33'$
number of formula units per unit cell	$z = 4$
cation site symmetry	$\text{La}^{3+} - C_1$ $\text{Be}^{3+} - C_1$
number of La^{3+} ions, (cm^{-3})	1.94×10^{22}
interatomic distances (Å)	$\text{La-O} = 2.415 - 2.999$ $\text{Be-O} = 1.602 - 1.678$ $\text{La-La} = 3.944 - 4.897$
(X-ray) density (g cm^{-3})	6.061
molecular weight	375.8
hardness (Knoop, 100 g load) (kg mm^{-2})	890 ($\parallel a$) 890 ($\parallel b$) 810 ($\parallel c$)
sound velocities (10^5 cm s^{-1})	$\parallel a$ axis (6.82) _l ; (3.82) _{fs} ; (3.52) _{ss} $\parallel b$ axis (6.88) _l ; (3.94) _{fs} ; (2.92) _{ss} $\parallel c$ axis (6.55) _l ; (3.70) _{fs} ; (3.48) _{ss}
ultrasonic attenuation for longitudinal wave propagation along the b -axis at 500 MHz ($\text{dB } \mu\text{s}^{-1}$)	0.5
elastic constants ($10^{12} \text{ dyn cm}^{-2}$)	$C_{22} = 2.87$ $C_{44} = 0.73$
melting point ($^\circ\text{C}$)	≈ 1400
thermal conductivity ($\text{W cm}^{-1} \text{ K}^{-1}$)	0.46 ($\parallel a$) 0.47 ($\parallel b$) 0.47 ($\parallel c$)
thermal expansion coefficients (from X-ray lattice constant measurements) (10^{-6} K^{-1})	7.0 ($\parallel a$) 7.9 ($\parallel b$) 9.5 ($\parallel c$) -0.9 (angle β)
refractive indices (at $1 \mu\text{m}$)	$n_x = 1.9641$ $n_y = 1.9974$ $n_z = 2.0348$
(at $1.3 \mu\text{m}$)	$n_x = 1.9566$ $n_y = 1.9896$ $n_z = 2.0262$
angle between the crystallographic axis c and the indicatrix axis z	$\rho = 31^\circ 30'$
optical transparency (μm)	0.22 - 5.4
nonlinear refractive index (10^{-13} e.s.u.)	$n_2 \approx 2.1$

Table 2

Intermanifold luminescence branching ratios $\beta_{JJ'}$ and $\beta_{JJ'}^{\text{or}}$ of $\text{La}_2\text{Be}_2\text{O}_5:\text{Nd}^{3+}$ crystals at 300 K

laser channel*)	$\beta_{JJ'}$	$\beta_{JJ'}^{\text{or}}$		
		crystallographic direction		
		a	b	c
${}^4\text{F}_{3/2} \rightarrow {}^4\text{I}_{11/2}$	0.552	0.496	0.576	0.584
${}^4\text{F}_{3/2} \rightarrow {}^4\text{I}_{13/2}$	0.125	0.118	0.133	0.123

*) $\beta_{JJ'} = 0.317$ for ${}^4\text{F}_{3/2} \rightarrow {}^4\text{I}_{9/2}$ transition and $\beta_{JJ'} = 0.006$ for ${}^4\text{F}_{3/2} \rightarrow {}^4\text{I}_{15/2}$ transition.

Table 3

Spectral characteristics and luminescence line intensities in the ${}^4\text{F}_{3/2} \rightarrow {}^4\text{I}_{11/2}$ transition of Nd^{3+} ions in $\text{La}_2\text{Be}_2\text{O}_5$ crystals at 77 and 300 K

wavelength (Å)	luminescence linewidth (cm^{-1})	β_{ij}^{or}	A_{ij}^{or} (s^{-1})	$\sigma_{e,ij}^{\text{or}}$ (10^{-19} cm^2)		
				crystallographic direction		
				a	b	c
77 K						
10694	5 ± 0.3	0.15	990	4.69	5.54	3.22
10740	17 ± 1.5	—	—	—	—	—
10785	9 ± 0.5	0.117	770	2.06	2.43	2.95
10858	9 ± 0.5	0.0526	350	0.95	1.08	1.33
10885	11 ± 1.0	0.0823	540	1.2	1.43	1.16
10990	16 ± 1.5	0.054	360	0.56	0.61	0.76
11080	11 ± 1.0	0.04	260	0.6	0.67	1.13
300 K						
10465	46 ± 4.0	0.0085	200	0.03	0.03	0.03
10553	56 ± 4.0	0.0218	520	0.06	0.07	0.09
10617	55 ± 4.0	0.024	570	0.07	0.08	0.07
10640	57 ± 4.0	0.031	740	0.08	0.1	0.09
10698	30 ± 3.0	0.0983	870	0.51	0.6	0.36
10749	75 ± 5.0	0.048	1140	0.1	0.11	0.12
10790	38 ± 4.0	0.0815	720	0.34	0.39	0.48
10827	55 ± 4.0	0.028	670	0.08	0.09	0.1
10857	38 ± 4.0	0.037	330	0.16	0.18	0.21
10880	39 ± 4.0	0.05	450	0.21	0.24	0.21
10995	53 ± 5.0	0.039	350	0.12	0.13	0.15
11075	38 ± 4.0	0.0284	250	0.12	0.14	0.22

ability determined as

$$A_{JJ'} = \frac{1}{3} \sum_{ij} \sum_{a,b,c} A_{ij}^{\text{or}},$$

where $A_{JJ'} = \beta_{JJ'}/\tau_{\text{rad}}$. Here τ_{rad} is the emission lifetime of the metastable ${}^4\text{F}_{3/2}$ state, $\Delta\nu_{\text{lum}}$ the luminescence line-width, b_i the i -th Stark level Boltzmann factor of the ${}^4\text{F}_{3/2}$ state relative to its first level ($i = 1$), $p_{ij}^{i_m j_m}$ are coefficients characterizing the overlapping of the neighbouring lines of the $i_m \rightarrow j_m$ transition with the line of a given $i \rightarrow j$ transition.

The relative values of orientationally dependent $\beta_{JJ'}$ and β_{ij}^{or} luminescence branching ratios were found according to the luminescence spectra, recorded along the three crystallographic directions a , b , and c and corrected for the sensibility of photoresistor and dispersion of SDL-1 spectrometer. Absolute values of $\beta_{JJ'}$ and β_{ij}^{or} were determined by (1), according to the determined values $\beta_{JJ'}$ and the relative values of the two coefficients mentioned above.

4. Experimental Results

The luminescence lifetime measured in a sample with low Nd^{3+} concentration (≈ 0.3 at%) is equal to (155 ± 10) μs and constant in a large temperature range (up to ≈ 700 K). This shows that the luminescence quantum yield from the ${}^4\text{F}_{3/2}$ levels

Table 4

Spectral characteristics and luminescence line intensities in the ${}^4\text{F}_{3/2} \rightarrow {}^4\text{I}_{13/2}$ transition of Nd^{3+} ions in $\text{La}_2\text{Be}_2\text{O}_5$ crystals at 77 and 300 K

wavelength (Å)	luminescence linewidth (cm^{-1})	β_{ij}^{or}	A_{ij}^{or} (s^{-1})	$\sigma_{e,ij}^{\text{or}}$ (10^{-19} cm^2)		
				crystallographic direction		
				a	a	b
77 K						
13503	5 ± 0.3	0.04	265	2.0	2.34	1.96
13647	9 ± 0.3	0.024	155	0.66	0.75	0.79
13763	10 ± 1.0	0.0115	75	0.29	0.31	0.29
13820	10 ± 1.5	0.0085	55	0.22	0.24	0.24
13980	16 ± 2.0	0.011	70	0.18	0.24	0.15
14135	16 ± 2.0	0.013	85	0.22	0.23	0.22
14240	17 ± 2.0	0.01	65	0.16	0.18	0.18
300 K						
13140	54 ± 4.0	0.004	100	0.02	0.025	0.015
13273	56 ± 4.0	0.0095	225	0.04	0.05	0.04
13382	56 ± 4.0	0.0118	280	0.05	0.06	0.06
13439	59 ± 4.0	0.0053	125	0.02	0.025	0.02
13510	36 ± 3.0	0.027	240	0.19	0.22	0.19
13591	68 ± 5.0	0.0063	150	0.02	0.03	0.025
13650	37 ± 3.0	0.017	150	0.12	0.14	0.14
13731	71 ± 7.0	0.0044	105	0.015	0.02	0.015
13765	39 ± 3.0	0.0076	70	0.05	0.05	0.05
13825	38 ± 3.0	0.005	45	0.035	0.035	0.035
13985	48 ± 5.0	0.0074	65	0.04	0.04	0.03
14137	50 ± 5.0	0.0073	65	0.04	0.045	0.04
14243	52 ± 5.0	0.005	45	0.03	0.03	0.03

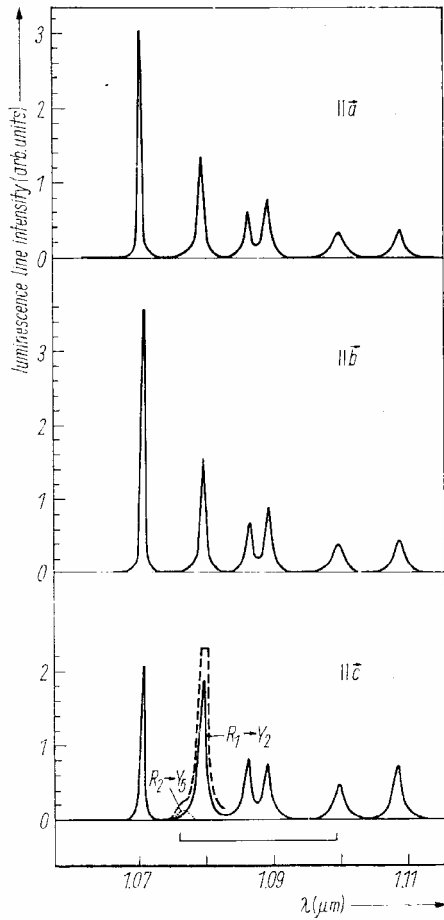


Fig. 1

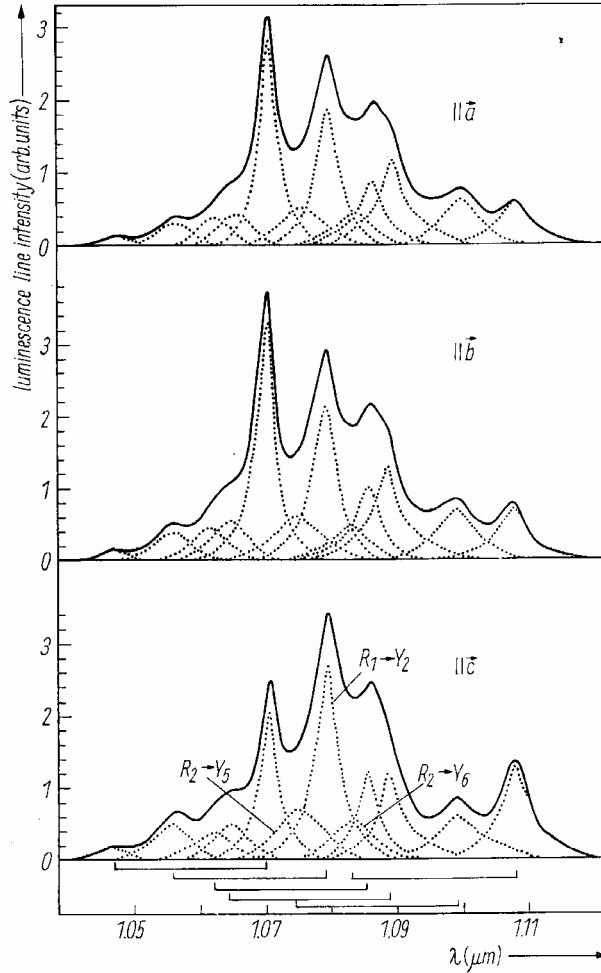


Fig. 2

Fig. 1. Orientational luminescence spectra (${}^4\text{F}_{3/2} \rightarrow {}^4\text{I}_{11/2}$) of Nd^{3+} ions in a $\text{La}_2\text{Be}_2\text{O}_5$ crystal at 77 K. The dashed curves show the results of decomposition of the complicated spectral contours. For explanations see text

Fig. 2. Orientational luminescence spectra (${}^4\text{F}_{3/2} \rightarrow {}^4\text{I}_{11/2}$) of Nd^{3+} ions in a $\text{La}_2\text{Be}_2\text{O}_5$ crystal at 300 K. Notations as in Fig. 1

is near unity, and hence $\tau_{\text{lum}} \approx \tau_{\text{rad}}$. The analysis of the absorption spectra in the ${}^4\text{I}_{9/2} \rightarrow {}^2\text{P}_{1/2}$ and ${}^4\text{I}_{9/2} \rightarrow {}^4\text{I}_{15/2}$ transitions gives an X parameter value ≈ 0.42 . The determined $\beta_{JJ'}$ values for the ${}^4\text{F}_{3/2} \rightarrow {}^4\text{I}_{11/2}$ and ${}^4\text{F}_{3/2} \rightarrow {}^4\text{I}_{13/2}$ transitions corresponding to the given X -value are listed in Table 2. Here the $\beta_{JJ'}^{\text{or}}$ coefficients measured by luminescence spectra are also presented. The values of $\Delta\nu_{\text{lum}}$, β_{ij}^{or} , A_{ij}^{or} , and $\sigma_{e,ij}^{\text{or}}$ for the ${}^4\text{F}_{3/2} \rightarrow {}^4\text{I}_{11/2}$ and ${}^4\text{F}_{3/2} \rightarrow {}^4\text{I}_{13/2}$ transitions are shown in Tables 3 and 4, respectively. The values of β_{ij}^{or} were measured by the luminescence spectra shown in Fig. 1 to 4. To prevent Tables 3 and 4 from being too bulky, values of β_{ij}^{or} and A_{ij}^{or} are given only for one crystallographic direction ($\parallel \mathbf{a}$). The values of orientational effective cross-sections σ_e^{eff} for the most intense luminescent lines related with laser performance were calculated by (3) and are given in Table 5. The data of Tables 2 to 5 and the spectra in Fig. 1 to 4 show that in spite of its low symmetry the $\text{La}_2\text{Be}_2\text{O}_5:\text{Nd}^{3+}$ crystal luminescence (unpolarized) anisotropy is weaker than that of some other

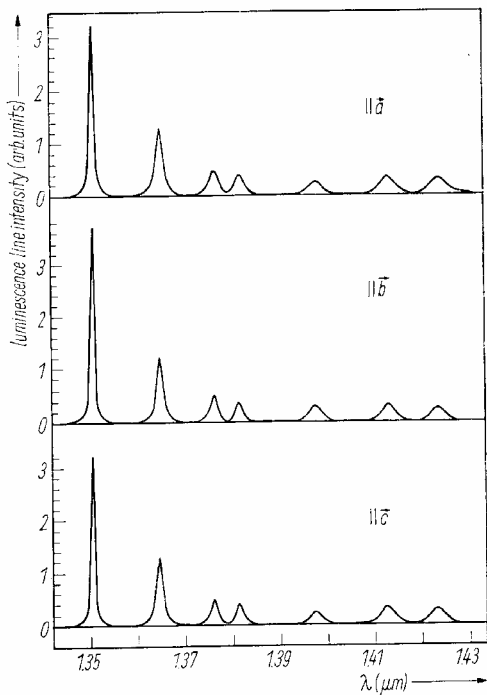


Fig. 3

Fig. 3. Orientational luminescence spectra (${}^4F_{3/2} \rightarrow {}^4I_{13/2}$) of Nd^{3+} ions in a $La_2Be_2O_5$ crystal at 77 K. Notations as in Fig. 1

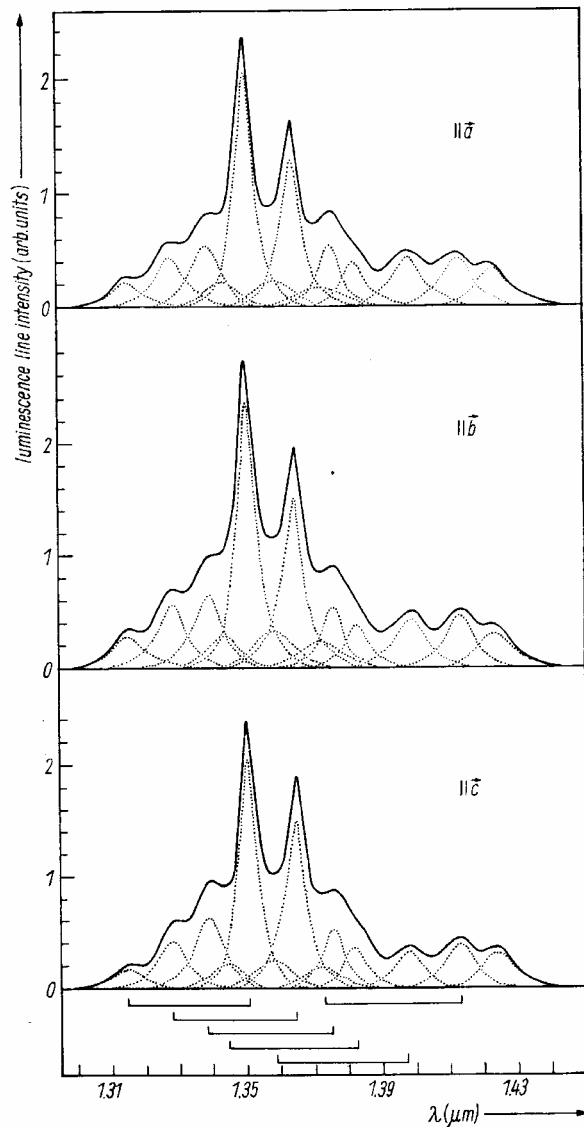


Fig. 4

Fig. 4. Orientational luminescence spectra (${}^4F_{3/2} \rightarrow {}^4I_{13/2}$) of Nd^{3+} ions in a $La_2Be_2O_5$ crystal at 300 K. Notations as in Fig. 1

crystals (for example, see results on orthorhombic $YAlO_3$ and monoclinic $KY(WO_4)_2$ and $KGd(WO_4)_2$ crystals with Nd^{3+} ions in [12, 15]). This agrees with the other physical characteristics of the $La_2Be_2O_5$ crystal given in Table 1. In the recent work [16] the weak anisotropy of the spectra for this crystal was also noted. Our results on the orientational luminescence investigations (along crystallographic axes a , b , and c) may be added to the data of [2], where polarized luminescence in the directions corresponding to the indicatrix axes of the $La_2Be_2O_5:Nd^{3+}$ crystal was studied. In the latter case a considerable luminescence line anisotropy for the ${}^4F_{3/2} \rightarrow {}^4I_{11/2}$ transition was observed.

Table 5

Effective cross-sections of some intense luminescence lines of $\text{La}_2\text{Be}_2\text{O}_5:\text{Nd}^{3+}$ crystals

laser channel	line wavelength (Å)	T (K)	σ_e^{eff} (10^{-19} cm 2)		
			crystallographic direction		
			$\parallel \mathbf{a}$	$\parallel \mathbf{b}$	$\parallel \mathbf{c}$
${}^4\text{F}_{3/2} \rightarrow {}^4\text{I}_{11/2}$	10694	77	4.69	5.54	3.22
	10785		2.06	2.43	2.95
	10698	300	0.57	0.68	0.45
	10790		0.47	0.53	0.62
${}^4\text{F}_{3/2} \rightarrow {}^4\text{I}_{13/2}$	13503	77	2.0	2.34	1.96
	13510	300	0.22	0.25	0.22

In our investigations Stark levels of the Nd^{3+} ion, the absorption transitions to which from the ground ${}^4\text{I}_{9/2}$ state correspond to the optical transparency band of the $\text{La}_2\text{Be}_2\text{O}_5$ crystal, were determined at 77 and 300 K. These data are given in Table 6.

In the present laser experiments the main problem was to investigate the temperature dependence of SE. The character of the SE temperature behaviour in the ${}^4\text{F}_{3/2} \rightarrow {}^4\text{I}_{11/2}$ transition lines of Nd^{3+} ions in the $\text{La}_2\text{Be}_2\text{O}_5$ ($\mathbf{F} \parallel \sim \mathbf{c}$) crystal is in good agreement with the luminescence spectra shown in Fig. 1 and 2. At 77 K generation is observed only at the short wavelength 1.0694 μm line, but at ≈ 80 K already at both line mentioned above and the longer wavelength 1.0785 μm line (see Fig. 5). As Fig. 5 shows, with further increase of temperature up to 300 K, generation occurs only at the longer wavelength, corresponding to the $\text{R}_1 \rightarrow \text{Y}_2$ line in the luminescence spectra (see Fig. 2, case $\parallel \mathbf{c}$). The mentioned feature of the SE temperature behaviour is explained by the presence of two lines $\lambda = 1.0749 \mu\text{m}$ and $\lambda = 1.0827 \mu\text{m}$, neighbouring with the $\text{R}_1 \rightarrow \text{Y}_2$ line and influencing its intensity in the emission spectrum of the $\text{La}_2\text{Be}_2\text{O}_5:\text{Nd}^{3+}$ ($\mathbf{F} \parallel \mathbf{c}$) crystal. These two neighbouring lines ($\text{R}_2 \rightarrow \text{Y}_5$ and $\text{R}_2 \rightarrow \text{Y}_6$, see Fig. 1 and 2) belong to the excited component (R_2) of the metastable

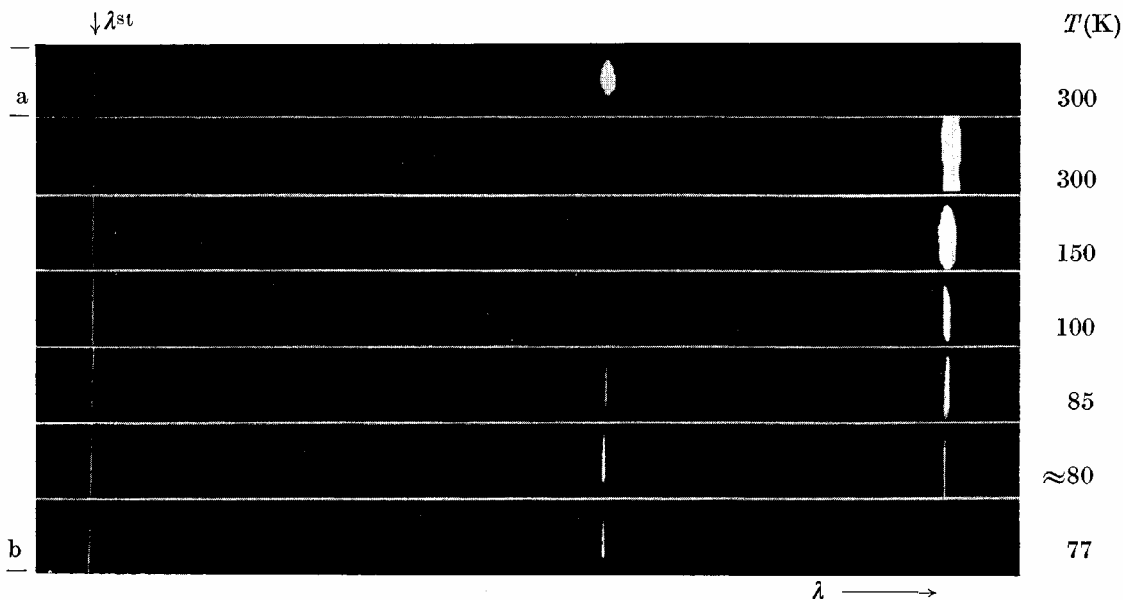


Fig. 5. SE temperature spectra of $\text{La}_2\text{Be}_2\text{O}_5:\text{Nd}^{3+}$ crystals. Standard line wavelength $\lambda_{\text{st}} = 10561 \text{ \AA}$. a) $\mathbf{F} \parallel \mathbf{a}$, b) $\mathbf{F} \parallel \mathbf{c}$

Table 6
The $4f^3 [S, L, J]$ manifold splitting of Nd^{3+} ions in $La_2Be_2O_5$ crystals at 77 and 300 K

S, L, J	level positions (cm^{-1})	component number		ΔE
		theor.	exper.	(cm^{-1})
77 K				
$^4I_{9/2}$	0, 110, 225, 350, 495	5	5	495
$^4I_{11/2}$	1961, 2040, 2102, 2125, 2213, 2287	6	6	326
$^4I_{13/2}$	3906, 3984, 4046, 4076, 4159, 4237, 4290	7	7	384
$^4I_{15/2}$	5820, 5933, 6003, 6090, 6210, 6298, 6395, 6495	8	8	675
$^4F_{3/2}$	11312, 11525	2	2	213
$^4F_{5/2} + ^2H_{9/2}$	12347, 12450, 12497, 12538, 12578, 12631, 12697, 12786	8	8	(439)
$^4F_{7/2} + ^4S_{3/2}$	13265, 13378, 13507, 13518, 13540, 13610	6	6	(345)
$^4F_{9/2}$	14565, 14661, 14715, 14801, 14889	5	5	324
$^2H_{11/2}$	15869, 15878, 15925, 15960, 16003, 16026	6	6	157
$^4G_{5/2}$	16954, 17034, 17108	3	3	154
$(^2G, ^4G)_{7/2}$	17221, 17261, 17302, 17355	4	4	134
$(^2G, ^4G)_{7/2}$	18851, 18911, 18938, 19016	4	4	165
$^2K_{13/2} + ^2G_{9/2}$	19143, 19358, 19373, 19415, 19464, 19512, 19618, 19692, 19800, 20023	12	10	(880)*
$^4G_{9/2} + ^4G_{11/2} + ^2K_{15/2} + ^2D_{3/2}$	20838, 20890, 20912, 20961, 20996, 21024, 21114, 21227, 21278, 21345, 21373*), 21398*), 21475, 21513, 21596, 21618, 21661, 21742, 21862, 22027	21	20	(1189)*
$^2P_{1/2}$	23126	1	1	—
$^2D_{5/2}$	23496, 23745*), 23954*)	3	3	458*)
$^2P_{3/2}$	25936, 25167*)	2	2	231*)
300 K				
$^4I_{9/2}$	0, 110, 225, 350, 495	5	5	495
$^4I_{11/2}$	1962, 2042, 2100, 2120, 2215, 2282,	6	6	320
$^4I_{13/2}$	3908, 3984, 4045, 4077, 4160, 4235, 4290	7	7	382
$^4F_{3/2}$	11310, 11518	2	2	208

*) These values of energy levels and total splitting of manifolds (ΔE) require more accurate definition. The total splitting of manifolds, the level separation of which is difficult, is taken in parantheses.

Table 7
Laser characteristics of $La_2Be_2O_5:Nd^{3+}$ crystals

laser channel	crystal orientation	T (K)	laser wavelength (\AA)	E_{thr} (J)
$^4F_{3/2} \rightarrow ^4I_{11/2}$	$F \parallel c$	77	10785	0.5
		85	10785	—
		300	10694	—
	$F \parallel a$	300	10790	3.0
		300	10698	1.8
$^4F_{3/2} \rightarrow ^4I_{13/2}$	$F \parallel a$	300	13510	2.5

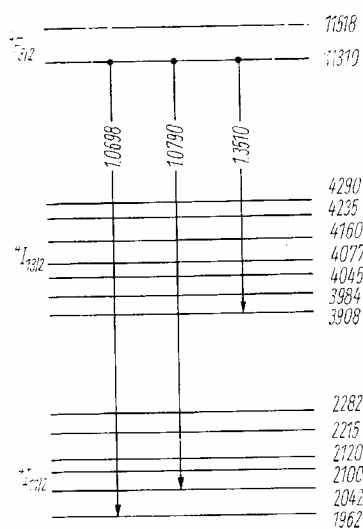


Fig. 6. Simplified scheme of Nd^{3+} ion levels in $\text{La}_2\text{Be}_2\text{O}_5$ crystals at 300 K. Thick arrows corresponding to laser transitions. The level positions are in cm^{-1} and transitions between them in \AA .

${}^4\text{F}_{3/2}$ state and broaden with temperature increase, rising in intensity due to the R_2 component Boltzmann population and hence overlapping with the laser $\text{R}_1 \rightarrow \text{Y}_2$ line. This results in the rise of the effective cross-section of the latter line. The results of laser measurements of the $\text{La}_2\text{Be}_2\text{O}_5:\text{Nd}^{3+}$ crystals are listed in Table 7, and the data of the identification of the registered induced transitions are shown in Fig. 6.

The study of the $\text{La}_2\text{Be}_2\text{O}_5:\text{Pr}^{3+}$ crystal absorption and luminescence spectra (see Fig. 7) was carried out as a first step of its investigations. The analysis of these spectra permitted us to determine the crystal-field splitting scheme of the Pr^{3+} ion manifolds, the transitions between the levels of which correspond to the optical transparency band of the $\text{La}_2\text{Be}_2\text{O}_5$ crystals. These data are given in Table 8. The experiments on SE excitation in the ${}^3\text{P}_0 \rightarrow {}^3\text{H}_6$ and ${}^3\text{P}_0 \rightarrow {}^3\text{H}_5$ transitions which gave negative results were also carried out at 77 K. The obtained information about the $\text{La}_2\text{Be}_2\text{O}_5:\text{Pr}^{3+}$ crystal properties allows us to consider it as a potential lasing medium.

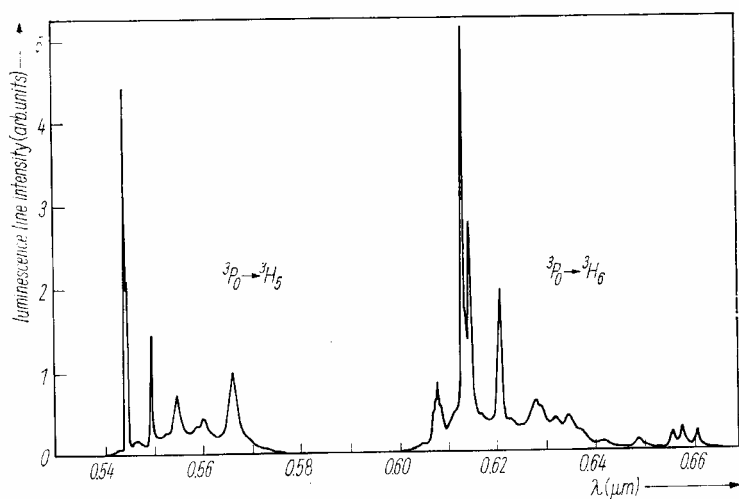


Fig. 7. Luminescence spectra (${}^3\text{P}_0 \rightarrow {}^3\text{H}_5$ and ${}^3\text{P}_0 \rightarrow {}^3\text{H}_6$) of Pr^{3+} ions in $\text{La}_2\text{Be}_2\text{O}_5$ crystal at 77 K

Table 8
The $4f^2$ [S, L, J] manifold splitting of Pr^{3+} ions in $\text{La}_2\text{Be}_2\text{O}_5$ crystals at 77 K

S, L, J	level positions (cm^{-1})	component number		ΔE (cm^{-1})
		theor.	exper.	
$^3\text{H}_4$	0, 6*), 25, 57, 165, 207, 543, 720, 771	9	9	771
$^3\text{H}_5$	2111, 2123, 2135*), 2175*), 2288, 2302*), 2456, 2576, 2635, 2832	11	10	721*)
$^3\text{H}_6$	4181, 4195, 4212, 4361, 4377, 4556, 4589, 4657, 4728, 4782, 4912, 5075, 5110	13	13	929
$^3\text{F}_2$	5172, 5226, 5239, 5282, 5348	5	5	176
$^3\text{F}_3$	6489, 6533, 6564, 6590, 6632, 6654, 6729	7	7	240
$^3\text{F}_4$	6944, 6962, 6989, 7052, 7082, 7103, 7145, 7205	9	8	261*)
$^1\text{G}_4$	9712, 9798, 9864, 9968, 10020, 10090, 10141, 10362	9	8	650*)
$^1\text{D}_2$	16495, 16718, 16934, 17028, 17094,	5	5	599
$^3\text{P}_0$	20500	1	1	—
$^3\text{P}_1$	20670, 20697, 20930	3	3	260
$^1\text{I}_6$	20986, 21037, 21109*), 21250, 21282*), 21314, 21344*), 21371*), 21429*)	13	9	443*)
$^3\text{P}_2$	22106, 22179, 22331*), 22527, 22590	5	5	484

*) These values of energy levels and total splitting of manifolds (ΔE) require more accurate definition.

Acknowledgements

The authors wish to express their thanks to V. V. Osiko and O. O. Bukin for support.

References

- [1] R. C. MORRIS, C. F. CLINE, R. F. BEGLEY, M. DUTOIT, P. J. HARGET, H. P. JENSSEN, T. S. LAFRANCE, and R. WEBB, *Appl. Phys. Letters* **27**, 444 (1975).
- [2] H. P. JENSSEN, R. F. BEGLEY, R. WEBB, and R. C. MORRIS, *J. appl. Phys.* **47**, 1496 (1976).
- [3] L. S. GOLDBERG and J. N. BRADFORD, *Appl. Phys. Letters* **29**, 585 (1976).
- [4] V. N. MATROSOV, M. I. TIMOSHECHKIN, E. G. TSVETKOV, S. E. SARKISOV, and A. A. KAMINSKII, *Digest of Technical Papers of V. All-Union Meeting Crystal Growth, Tbilisi 1977*, Vol. 2 (p. 167) (in Russian).
- [5] C. E. WEIR and A. VAN VALKENBURG, *J. Res. Nat. Bur. Standards* **A64**, 105 (1960).
- [6] L. A. HARRIS and H. L. YAKEL, *Acta cryst.* **B24**, 672 (1968).
- [7] YU. K. VORONKO, G. V. MAKSIMOVA, V. V. OSIKO, A. A. SOBOL, B. P. STARIKOV, and M. I. TIMOSHECHKIN, *phys. stat. sol. (a)* **17**, K41 (1973).
- [8] C. F. CLINE and R. C. MORRIS, U.S. Patent No. 3.866.142, Febr. 11, 1975.
- [9] W. L. SMITH and H. BECHTEL, *Appl. Phys. Letters* **28**, 606 (1976).
- [10] A. A. KAMINSKII and L. LI, *phys. stat. sol. (a)* **26**, 593 (1974).
- [11] A. A. KAMINSKII and L. LI, *Zh. tekhn. Fiz., Pisma* **1**, 567 (1975).
- [12] A. A. KAMINSKII, S. E. SARKISOV, I. V. MOCHALOV, L. K. AMINOV, and A. O. IVANOV, *phys. stat. sol. (a)* **51**, 509 (1979).
- [13] A. A. KAMINSKII, *Zh. eksper. teor. Fiz.* **58**, 407 (1970).
- [14] A. A. KAMINSKII, A. O. IVANOV, S. E. SARKISOV, I. V. MOCHALOV, V. A. FEDOROV, and L. LI, *Zh. eksper. teor. Fiz.* **71**, 984 (1976).
- [15] A. A. KAMINSKII, S. E. SARKISOV, A. A. PAVLYUK, and V. A. LYUBCHENKO, *Izv. Akad. Nauk SSSR, Ser. neorg. Mater.* **16**, 720 (1980).
- [16] T. S. LOMHEIM and L. G. DE SHAZER, *Phys. Rev. B* **20**, 4343 (1979).

(Received February 1, 1980)